ADVANCES IN FOREST FIRE RESEARCH

2022

Edited by
DOMINGOS XAVIER VIEGAS
LUÍS MÁRIO RIBEIRO

Atmospheric turbulent structures during shrub fires and implications for flaming zone behavior

Marwan Katurji*[1]; Bob Noonan[1]; Jiawei Zhang[1,3]; Andres Valencia[2]; Benjamin Shumcher[1]; Jessica Kerr[3]; Tara Strand[3]; Grant Pearce[3,4]; Peyman Zawar-Reza[1]

[1]School of Earth and Environment, University of Canterbury, New Zealand, {marwan.katurji@canterbury.ac.nz}
[2]Dept. Of Civil and Natural Resources Engineering, University of Canterbury, New Zealand
[3]New Zealand Forest Research Institute, Scion, New Zealand
[4]Fire Emergency New Zealand- FENZ

**Corresponding author*

Keywords

Atmosphere, turbulence, fire observations, flaming zone

Abstract

Wildfires propagate across vegetated canopies exhibiting complex spread patterns. Wind gusts at the fire-front extend/intensify flames and direct convective heating towards unburnt fuels resulting in rapid acceleration of spread. This behavior could be modulated by ambient atmospheric boundary layer wind turbulence. Our aim is to characterize ambient turbulence over gorse shrub experimental burns and explore how this contributes to fire behavior. Developing coupled fire-atmosphere numerical models capable of resolving most turbulent energy scales is important for understanding rapid and small-scale dynamics. However, it is equally as important to design fire-burn experiments that allow for simultaneous measurements of fire behavior and atmospheric turbulence covering a range of the turbulent spectra. We have completed six experimental burns (24-hectares) in Rakaia, New Zealand under varying wind speed and direction and atmospheric stability regimes. The ignition process ensured a fire-line propagating through dense gorse bush (1m high). Two 30m high sonic anemometer towers measured turbulent wind velocity (20Hz) at six different height levels. Visible imagery was captured for all burns by cameras mounted on Un-crewed Aerial Vehicles (UAV) at 200m AGL. Using wavelet decomposition, we identified different turbulent scales that varied relative to height above vegetation and boundary layer thermal regimes. Quadrant analysis identified statistical distribution of atmospheric sweeps (downbursts of turbulence towards vegetation) and ejections (detachment of turbulence from vegetation). Discrete analysis of sweep/ejection events revealed their temporal and spatial scales and tracked their progression as the flaming zone approached the towers. Undergoing work aims to discern these interactions with observed fire sweeps from aerial imagery by applying image velocimetry techniques and sweep structure tracking.

1. Introduction

Turbulence is a ubiquitous property of the Atmospheric Boundary Layer (ABL) that extends up to 1 or 2km above ground level. ABL turbulence modulates how the near-surface atmosphere interacts with the anomalous/introduced energy perturbations caused by wildfires over timescales of minutes to hours (Stull, 1988). Closer to the surface, turbulent processes control heat, momentum and moisture transport between vegetated surfaces and the overlying Atmospheric Surface Layer (ASL) that extends between 100 and 200m above the surface and strongly influenced by wind shear or mechanically induced turbulence (LeMone et al. 2018). Wildfires produce positively buoyant turbulent motion that can lead to significant downward surges of momentum, interacting with ASL turbulence and potentially modulating a fire's rate of spread over short periods of time. (Heilman et al. 2019; Cunningham & Linn, 2007; Sun et al. 2009). Identifying these processes and studying their characteristics under environmental conditions can lead to better understanding erratic fire behavior.

Experimental field scale fires designed to measure turbulent flux at the fire-atmosphere interface can provide insights into the atmospheric processes controlling fire behavior. These experiments include in-situ tower-mounted sonic anemometer measurements from spreading fires in low grass to higher canopy fuels (Clements

et al., 2006, 2007, 2008; Heilman et al. 2019). Sonic anemometry allows for the ability of measuring 3-dimensional wind velocity, air temperature and humidity at high sampling rate, and quantifying momentum and moisture fluxes between the fire and the integral atmospheric scales measured across an averaging interval. Conclusions are then made regarding the amount of energy exchanged between the fire and the overlying atmosphere, the role of near-surface environmental shear and static stability on fire behavior (Potter, 2012). Other studies (Heilman et al., 2015, 2019) carried out measurements of vertically distributed turbulent heat and momentum flux during a surface fire progressing under 23m high pine trees. Their results confirmed that the largest enhancement of vertical turbulent flux happens at or above canopy levels. Spectral analysis of momentum and heat flux suggested that fire-atmosphere interactions can happen across a wide range of frequencies and further studies are needed to assess how those fluxes feedback into fire behavior. Complex vegetation cover, including spatial density variations, forest gaps and edges, and steep topography will produce spatially complex turbulent interactions. The presence of dense vegetation acts to increase wind shear and the production of turbulent kinetic energy, reduce the mean wind speed and increase gusts, and enhance vertical motion allowing for enhanced downward momentum transfer from the atmospheric surface layer (Kiefer et al. 2018; Schlegel et al. 2012, 2015).

The impact of atmosphere driven momentum surges on fire behavior has not been extensively studied. For grass fires, we now can hypothesize that convective heating pulses originating from the flaming zones are responsible for fuel heating and could play a large role in fire spread in any direction along the fire line (Cunningham & Linn, 2007). These processes have been (Cunningham & Linn, 2007) modelled by couple LES atmospheric-fire models like FIRETEC and observed in laboratory experiments (Finney et al., 2015; Tang et al., 2019). Turbulent flaming zone dynamics can now be observed using thermal image velocimetry techniques for real landscape scale experiments (Katurji et al., 2021), and have been shown to be related to overlying wind turbulence spectra. However, the role of atmospheric source momentum downward surges and their associated turbulence structures have not been studied in relation to fire horizontal convective heating dynamics. In this paper we present observations of characterized atmospheric turbulence strictures over a fast-spreading shrub fire and discuss their implication on fie behavior.

2. Methodology

2.1. Experimental Burn Design

The experimental burn layout is shown in Figure 1 and included 4 burn blocks hereafter referred to as plots P1, P2, P3, and P4. The experiments were carried out on the 2nd and 6th of March 2020 in the Rakaia Valley in New Zealand. Plots 3 and 4 were instrumented with a 30m sonic anemometer tower shown in Figure 1 and instrument setup details are shown in Table 1. The two towers were nearly centered in the burn blocks while the fire line and flaming zone passed across the towers.

Table 1. Observational systems and corresponding measurement parameters and specifications

Observational System	**Instrument**	**Accuracy, range (sensitivity, resolution)**	**Measured variable**	**Installation details**
Nadir visible video acquisition	Video camera (DJI Ltd.12MP RGB)	100m AGL 1920 x 1080 pixels Spatial resolution (pixels/m)	Visible video at 30fps	On Un-crewed Aerial Vehicle (UAV)
In-fire wind turbulence tower	Applied Technologies, Inc. 3-dimensional ultrasonic anemometer – SATI/3(K) series, Campbell Scientific CR6 datalogger	K-probe - 150 mm vertical and horizontal measurement path length. Sampling frequency 20Hz	U (+ve towards east), V (+ve towards north), W (+ve vertically upwards) [ms^{-1}]	1.6m (6h, 6.4h), 5m (18.9h, 20h), and 10m (37.7h, 40h) AGL and perpendicular to fire line

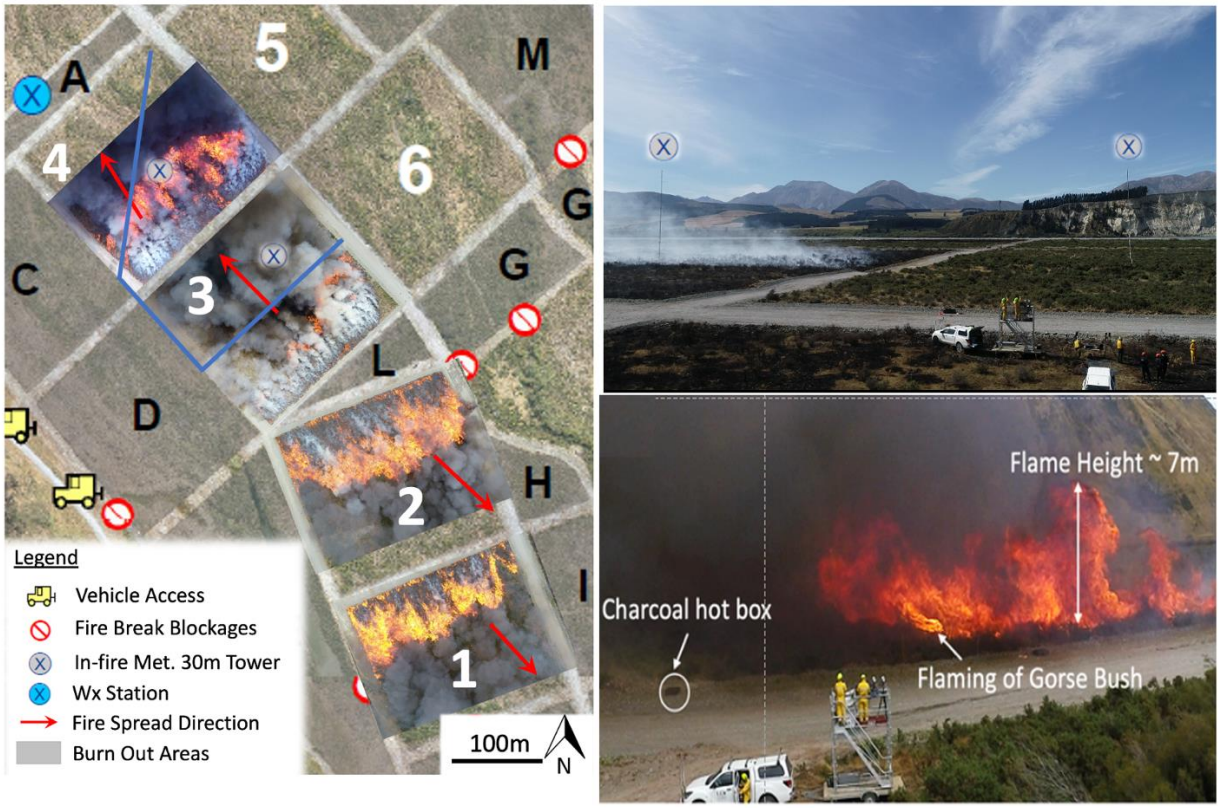

Figure 1- Experimental burn layout showing plot layout, fire spread direction and some site pictures The top view pictures of the flaming zone were taken from a UAV and overlaid on the map at the 2-minute point after the ignition of each plot

2.2. Data Processing

Data de-spiking, sonic tilt and orientation corrections were carried out on the sonic anemometer data – as in Katurji et al. (2021). The streamwise (U), velocity component was then geometrically projected to align with the mean wind direction for all the plots. Aerial video data was collected from nearly 200m above the plots.

2.3. Atmospheric Turbulence Analysis

2.3.1. Wavelet Transform

This study used the python package PYCWT to calculate the wavelet transform for time frequency analysis. Unlike Fourier transform, wavelet transform reserves the temporal information alongside the frequency information and is more suitable to look at the temporal variations of coherent structures in the turbulence time series from the streamwise and vertical wind velocity.

2.3.2. Quadrant Analysis

Wavelet transform can give temporal coherency information at difference frequency scales, but the method cannot distinguish different types of turbulent coherent structures. These involve “ejection motion” associated with turbulent eruption of low momentum streaks away from the surface; “sweep motion” or deceleration of the flow caused by the turbulent motion towards the surface; “outward motion” associated with the acceleration of the flow away from the surface due to low-level convergence; and “inward motions” associated with deceleration of the flow moving towards the surface due to low-level divergence (Christen et al., 2007; Li & Bou-Zeid, 2011; Wallace, 2016). The quadrant analysis in this study uses the instantaneous product of the streamwise (u′) and vertical velocity (w′) perturbations. For momentum flux, if we plot the velocity component pair (u′w′) into the Cartesian plane (abscissa for w′ and ordinate for u′), the first (I) quadrant (+w′-u′) will be outward quadrant while II, III and IV would be sweep, inward and ejection respectively (a sample from the tower data shown in Figure 2.

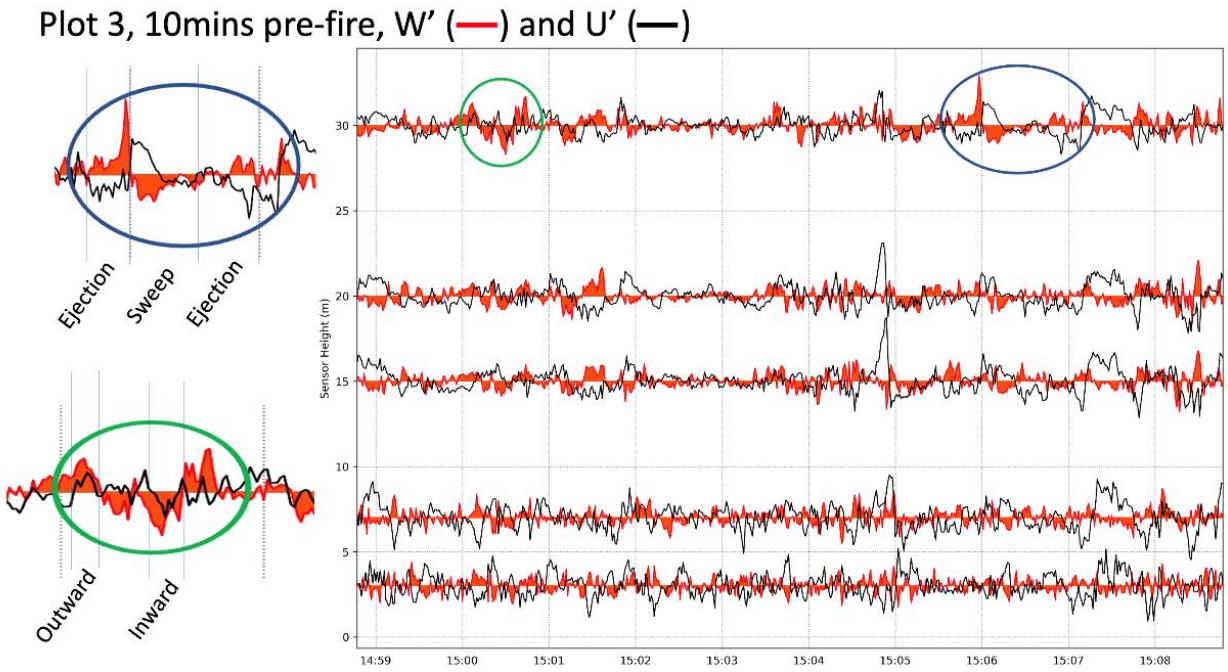

Figure 2- Vertical (streamwise) velocity perturbations from the 30m tower in plot 3. 20Hz perturbations were calculated from a 1-min rolling average window then subsampled with a 1s window average. Examples of sweep, ejection, inward, and outward motions are extracted in the left panel.

2.4. Flaming Zone Observation and Image Velocimetry

Image Velocimetry (IV) (Katurji et al. 2021) was applied on UAV overhead fire videos in order to derive and map the displacement of flame structures shown later in Figure 7. These structures manifest as diverging flame streaks that ignite fuel (example shown in Figure 3b, c). It was found that first-order physical characteristics of the observed fire sweeps, namely divergent fire flow from a near static center, were successfully captured and represented using IV. The ability of image velocimetry to capture physical characteristics of the fire sweeps was leveraged to develop a methodology capable of identifying fire sweeps from overhead UAV videos. This methodology applies a 2D convolution on the displacement vector field, and uses a kernel carefully designed to highlight the characteristics of fire sweeps spatially and temporally. The resultant scalar field represents a 2D map of the likelihood of occurrence of fire sweep, which is mainly limited by the size of the kernel and by the difficulty to calibrate it other than by visual inspection.

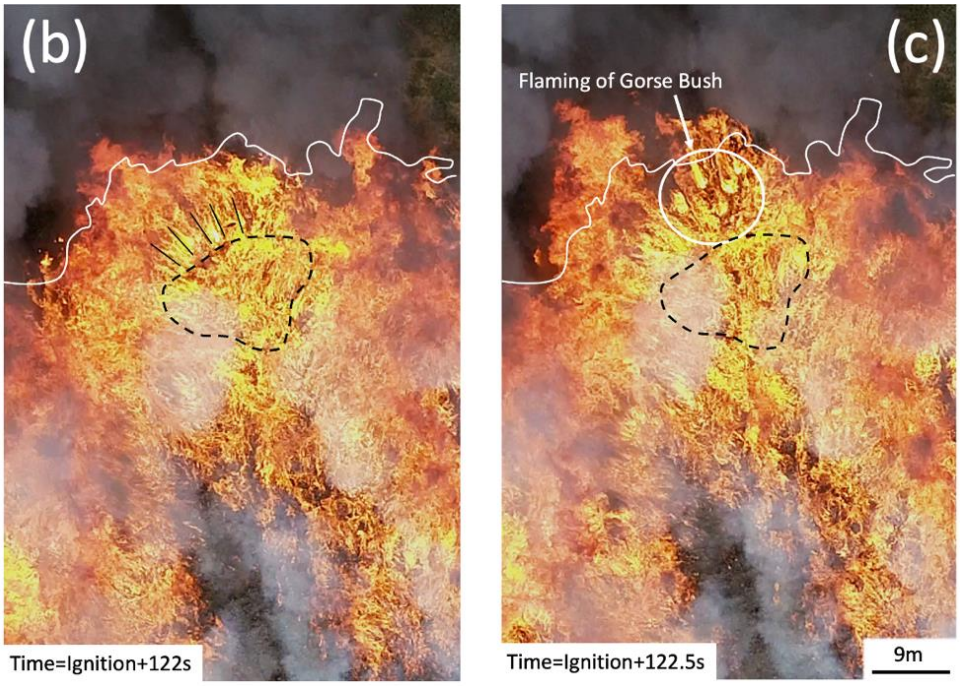

Figure 3- Observed flaming zone from nearly 200m AGL using a UAV. The black dotted outline in (b) and (c) shows the area of a fire "sweep" and its impact on vegetation ignition.

3. Results and Discussion

3.1. Meteorological and Burn Conditions

Burn events for plots 3 and 4 were associated with a typical up-valley afternoon air flow up to 1.5 ºC fluctuations in air temperature associate with the convective boundary layer (see third panel of Figure 4). Plots 1 and 2 were conducted under a synoptically driven nor-wester wind regime that produced orographically channeled down-valley winds, and warmer and drier air conditions as the airflow descended from the New Zealand Southern Alps towards the Rakaia valley. The burn time for all plots varied between 3 and 5 mins with an initial straight-line ignition and a wind driven flaming process.

Table 2. Fire behavior, and meteorological conditions (averaged over duration of burns) recorded at from the weather station tower marked by a blue circled "x" in Figure 1

Plot	Ignition time (plot edge reached) [NZDT]	Tair [°C] (RH) [%]	Wind speed [ms^{-1}] (direction) [°]	Mean gorse height [m]	Pre-burn gorse (grass, litter, debris) fuel load [kg m^{-2}]	Total fuel consumption [kg m^{-2}]	Rate of spread [m/s]	Flame height [m]
P1	02/03/2020, 10:10 (10:14)	20.7, (36)	8.27 (310)	0.83	1.8 (0.1,0.7,0.8)	2.5	0.89	4.9
P2	02/03/2020, 12:11 (12:14)	22.9, (33)	9.8 (311)	1.10	4.1 (0.3,1.3,1.7)	6.7	0.92	3.7
P3	06/03/2020, 15:08 (15:12)	21.6, (41)	6.8 (146)	0.84	2.2 (0.2,0.6,0.4)	2.4	0.9	5.4
P4	06/03/2020, 13:31 (13:36)	20.0, (43)	5.0 (142)	0.85	2.5 (0.7,0.7,1.0)	3.4	0.75	5.6

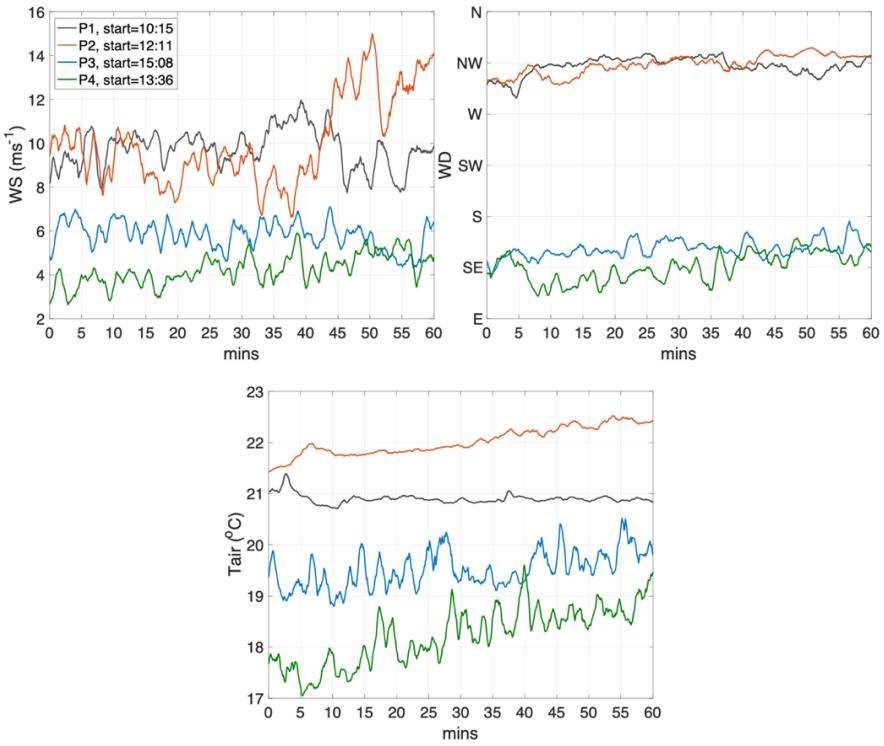

Figure 4- Time series of wind speed (WS), direction (WD), and air temperature (Tair) for 1-hour pre-fire at 30m AGL and 1min average interval. Plots 1 (P1), P2, P3, and P4 are shown indifferent colors with the start time hh:mm in NZDT indicated for each

3.2. Wind Turbulence Spectra

For all the plots, the integral time scales (usually detected when a power peak is evident) of turbulent wind velocity appear to get shorter as the measurement gets closer to the canopy (Figure 5), which is in accordance with boundary-layer turbulence theory. For heights less than 15m, where the observed flame heights (Table 2) occurred between 3 and 6 m, the results suggest that the energetic turbulent motion along the streamwise wind direction can occur between 2 and 32s. These results also show that the turbulent time scales vary between the atmospheric stability regimes of plots P1 and P2 compared to P3 and P4. Results from the vertical wind spectra, not shown in this extended abstract, reveal much shorter integral time scales for P1 and P2 (around 1 s) compared to P3 and P4 (between 3 and 5 s) when atmospheric turbulence was largely dominated by a thermal regime as opposed to the wind shear dominated regime of P1 and P2.

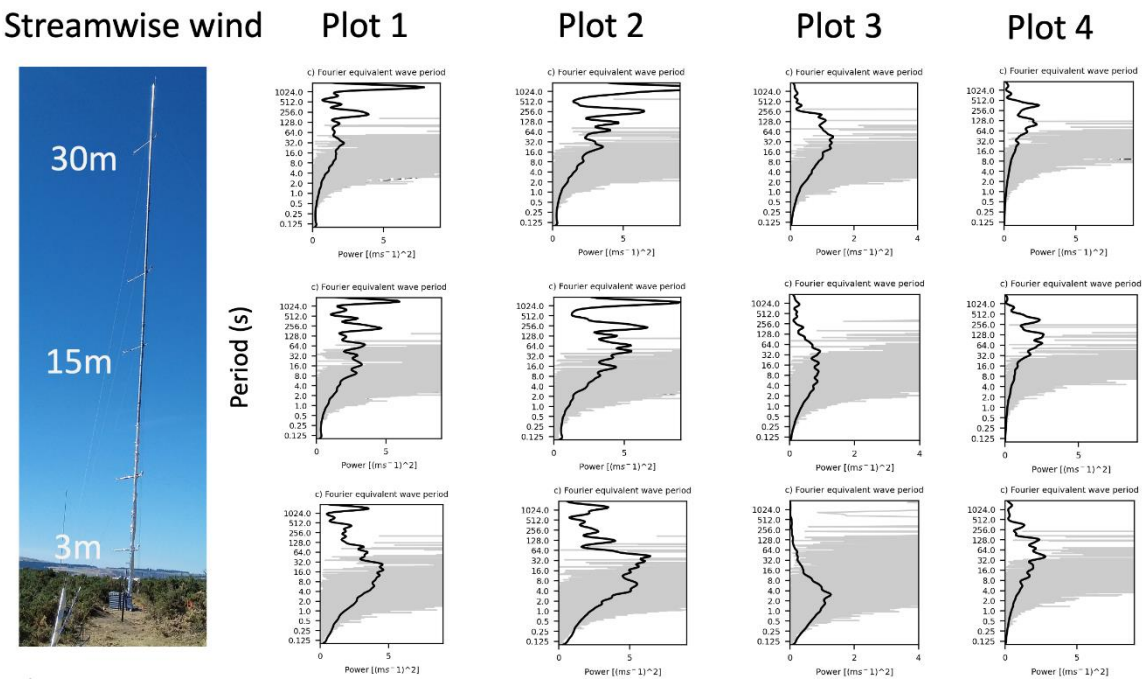

Figure 5- Black line shows the time integrated spectra across the wavelet time frequency decomposition showing the integral time scales (period on the y-axis) versus spectral power (on x-axis) for plots 1, 2, 3, and 4 and for three selected height levels on the tower (3, 15, and 30m). The gray line shows the Fast Fourier decomposition inserted for reference but not used in the analysis.

3.3. Atmospheric Sweep, Ejection, Inward and Outward Motions

Atmospheric turbulent structures plotted against time for all the plots (Figure 6) show more sweep and ejection events than inward and outward events. It has been previously suggested that coherent sweep (gust) and ejection (burst) motions dominate near-surface momentum and scalar fluxes(Li & Bou-Zeid, 2011). The reduction of the number of inward and outward motions for P1 and P2 compared to P3 and P4 does support the earlier findings of the integral time scale difference between the shear driven surface layer condition of P1 and P2 and the thermally driven surface layer turbulent motion of P3 and P4. Forward slanting coherence of sweep and ejection structures (highlighted in yellow - Figure 6) across the 30m tower height suggest that events can originate from within the surface layer (above the observed 30m roughness boundary layer) and impinge on the surface. These types of interactions will have a time scale associated with them (the width of the black boxes) and are being investigated as part of the ongoing work for this research. These events can be significant as it is our hypothesis that fire "sweeps", explained in the following section, can be impacted by these atmospheric turbulent structures by prolonging their duration and/or expanding the flame-vegetation interaction zone.

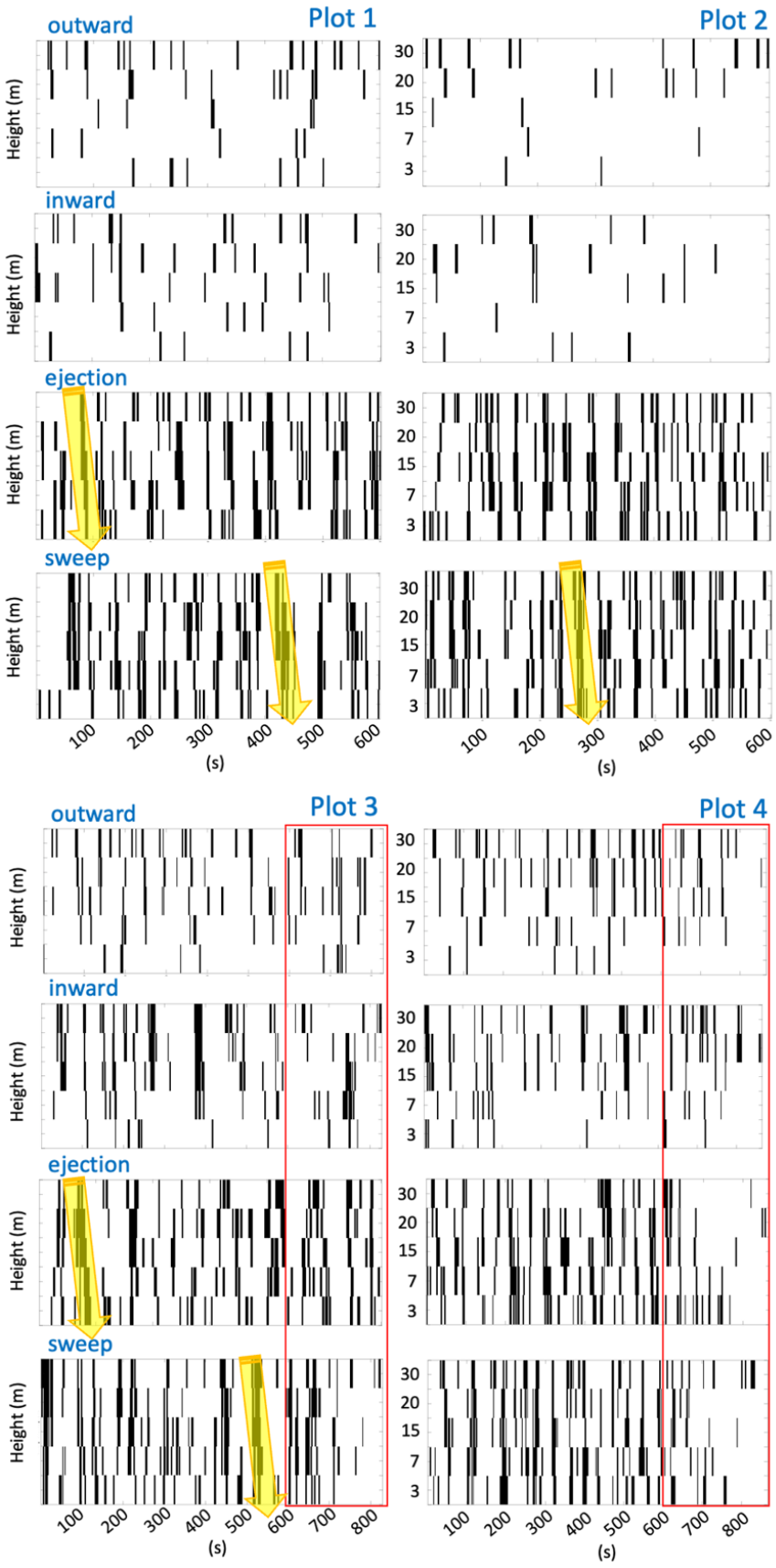

Figure 6- Sweep, ejection, inward and outward events detected at all the 5 height levels of the in-situ tower for plots 1, 2, 3 and 4. The red outlined box shows the period when the fire was progressing through plots 3 and 4. The yellow arrows show examples of downwards propagating structures

3.4. Flaming Zone and Fire Sweep Observations

UAV overhead visible video of the gorse vegetation fire carried out in P2 were selected for this preliminary analysis. Figure 7 highlights the observable flaming zone and some of its main features during the steady-state phase of the fire spread. The flaming zone dynamics was characterized by intermittent "fire bursts" in which clusters of unburned fuel were covered by the fire and ignited. Fire bursts were typically accompanied by strong tilting of the flame front inducing, in most of the cases, direct flame impingement.

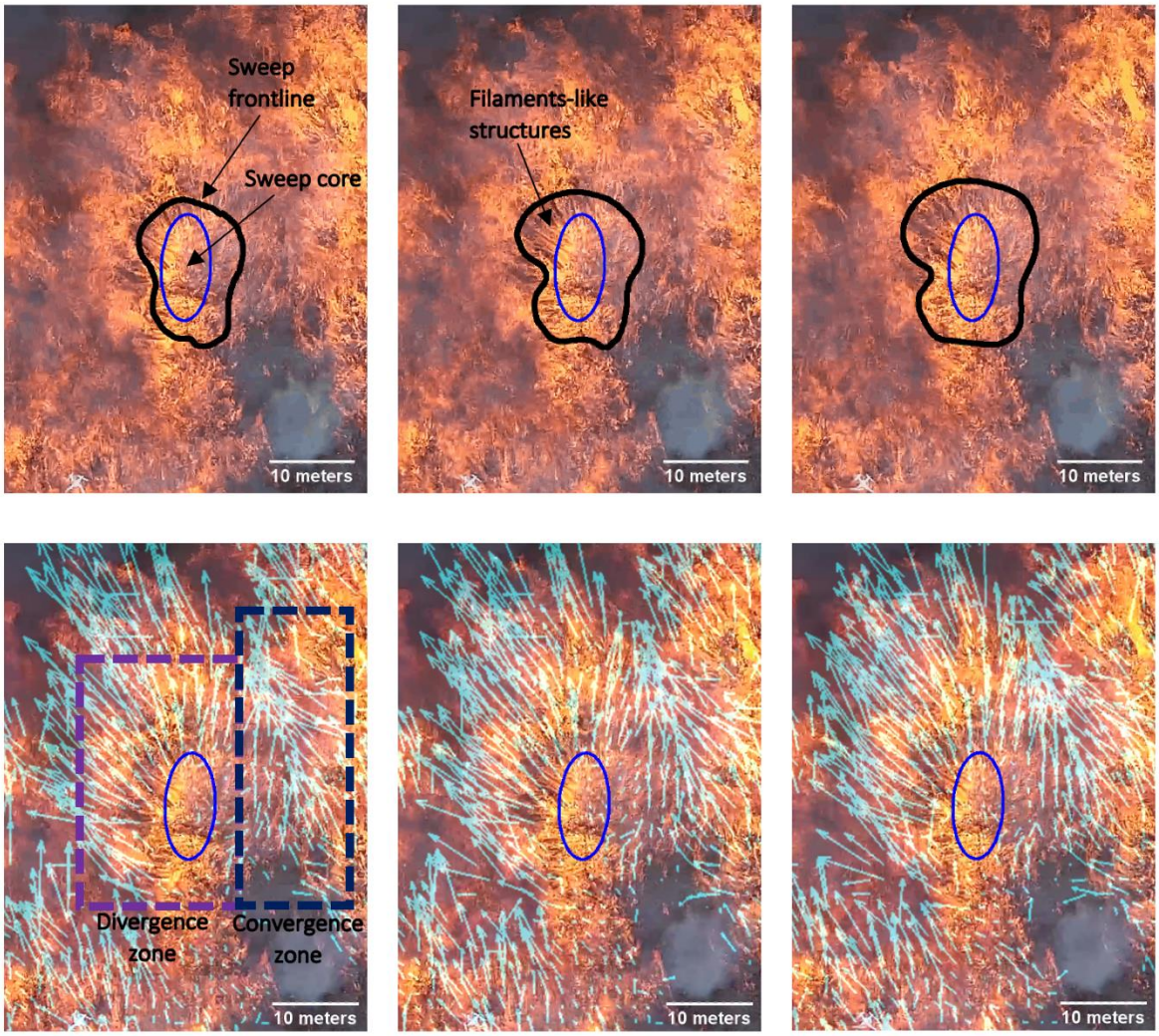

Figure 7- Time sequenced (at 1/30 s interval) frames extracted from the UAV video recorded during the P2 burn and an example of the resulting image velocimetry of identified fire sweep" events"

The structures in Figure 7, are referred to as *fire sweeps*, and are characterized by divergent motion of fire (or *fire sweep frontline*, black line) from a nearly static luminous region (or *fire sweep core*, region inside blue line). Structures with these characteristics were identified sporadically at multiple locations into the flaming zone. Generally, they were found to have a characteristic length of ~ 10 m during the incipient stage up to ~20-30 m during its peak. High luminosity inside the core region of the fire sweeps can last several seconds, and is recurrently accompanied with filament-like fire structures located around the it, which are characterized by divergent motion of the fire with higher spatiotemporal frequency. Inspection of side-view UAV footage (not shown here) suggests that tilted flames from individual bushes located near the core region are at the origin of these structures. Preliminary results from 2D convolution approach was used to track individual fire sweeps and estimate their duration. Two main groups of fire sweeps were identified. The first group is characterized by short-duration structures (< 1 s), generally quickly appearing and disappearing sporadically with short displacement through the flaming zone. Fire sweeps of the second group presented longer durations (up to 4 s) and were observed to move across the flaming zone, some of them from the back to the head of the fire.

4. Conclusion and Ongoing Work

Experimental fire observations included turbulent wind velocity measurements from a 30m tower and UAV-based video in nadir from nearly 200m above the flaming zone. The methods focussed on characterizing the overlying atmospheric turbulence strutcure, Image Velocitmetry (IV) and feature tracking of *fire sweeps*. More IV is planned and will be used to derive and map the displacement of *fire sweeps* and their durations and will be compared with statistical distribution of atmospheric turbulent motions and their durations.

The observations from the gorse aerial imaging of the flaming zone and some of the *fire sweep* processes are similar to the results of the numerical modelling of a spreading fire using FireTec (Cunningham & Linn, 2007). Their simulations included wind speed ranges similar to the conditions of the gorse fire experiment but without atmospheric boundary layer turbulence. The fire produced a series of regular streamwise vortices with flame buoyancy lifting air along the updraft lines and descending between two flaming corridors causing a *fire sweep*. The scale of one of the fire sweep in the Firetec simulations was between 10 and 20m, which is not very dissimilar to the scales we analyzed in this study.

5. Acknowledgements

We would like to give a special thanks to all field support teams including technical and general staff. We also thank landowner for their various contributions leading to the success of the field campaigns. University of Canterbury atmospheric research team would like to acknowledge the very thoughtful, well organized, and proactive support we have received from all the volunteering firefighting crew. The success of our experiments and the safety of our science crew can only be partially attributed to our design but greatly attributed to the safe and well-executed plan from the volunteer crew. A special thanks to the Scion UAV crew: Robin Hartley and Peter Massam. This research was co-funded by Ministry of Business, Innovation and Employment (MBIE), New Zealand, grant number C04X1603 and C04X2103.

6. References

Christen, A., Gorsel, E. van, & Vogt, R. (2007). Coherent structures in urban roughness sublayer turbulence. *International Journal of Climatology*, *27*(14), 1955–1968. https://doi.org/10.1002/joc.1625

Cunningham, P., & Linn, R. R. (2007). Numerical simulations of grass fires using a coupled atmosphere-fire model: Dynamics of fire spread. *Journal of Geophysical Research: Atmospheres (1984–2012)*, *112*(D5). https://doi.org/10.1029/2006jd007638

Finney, M. A., Cohen, J. D., Forthofer, J. M., McAllister, S. S., Gollner, M. J., Gorham, D. J., et al. (2015). Role of buoyant flame dynamics in wildfire spread. *Proceedings of the National Academy of Sciences*, *112*(32), 9833–9838. https://doi.org/10.1073/pnas.1504498112

Heilman, W. E., Bian, X., Clark, K. L., & Zhong, S. (2019). Observations of Turbulent Heat and Momentum Fluxes During Wildland Fires in Forested Environments Observations of Turbulent Heat and Momentum Fluxes During Wildland Fires in Forested Environments. *Journal of Applied Meteorology and Climatology*. https://doi.org/10.1175/jamc-d-18-0199.1

Hunt, K. M. R., Zaz, S. N., & Romshoo, S. A. (2021). Linking the North Atlantic Oscillation to winter precipitation over the Western Himalaya through disturbances of the subtropical jet. *Earth and Space Science Open Archive*, 13. https://doi.org/10.1002/essoar.10508131.1

Heilman, W. E., Clements, C. B., Seto, D., Bian, X., Clark, K. L., Skowronski, N. S., & Hom, J. L. (2015). Observations of fire-induced turbulence regimes during low-intensity wildland fires in forested environments: implications for smoke dispersion. *Atmospheric Science Letters*, *16*(4), 453–460. https://doi.org/10.1002/asl.581

Katurji, M., Zhang, J., Satinsky, A., McNair, H., Schumacher, B., Strand, T., et al. (2021). Turbulent Thermal Image Velocimetry at the Immediate Fire and Atmospheric Interface. *Journal of Geophysical Research: Atmospheres*, 126(24). https://doi.org/10.1029/2021jd035393

Kiefer, M. T., Heilman, W. E., Zhong, S., Charney, J. J., & Bian, X. (2016). A study of the influence of forest gaps on fire-atmosphere interactions. *Atmospheric Chemistry and Physics Discussions*, 1–23. https://doi.org/10.5194/acp-2015-933

Kiefer, M. T., Zhong, S., Heilman, W. E., Charney, J. J., & Bian, X. (2018). A Numerical Study of Atmospheric Perturbations Induced by Heat From a Wildland Fire: Sensitivity to Vertical Canopy Structure and Heat Source Strength. *Journal of Geophysical Research: Atmospheres*. https://doi.org/10.1002/2017jd027904

LeMone, M. A., Angevine, W. M., Bretherton, C. S., Chen, F., Dudhia, J., Fedorovich, E., et al. (2018). 100 Years of Progress in Boundary Layer Meteorology. *Meteorological Monographs, 59*, 9.1-9.85. https://doi.org/10.1175/amsmonographs-d-18-0013.1

Li, D., & Bou-Zeid, E. (2011). Coherent Structures and the Dissimilarity of Turbulent Transport of Momentum and Scalars in the Unstable Atmospheric Surface Layer. *Boundary-Layer Meteorology*, *140*(2), 243–262. https://doi.org/10.1007/s10546-011-9613-5

Potter, B. E. (2012). Atmospheric interactions with wildland fire behavior – I. Basic surface interactions, vertical profiles and synoptic structures. International Journal of Wildland Fire, 21(7), 779–801. https://doi.org/10.1071/WF11128

Sun, R., Krueger, S. K., Jenkins, M. A., Zulauf, M. A., & Charney, J. J. (2009). The importance of fire–atmosphere coupling and boundary-layer turbulence to wildfire spread. International Journal of Wildland Fire, 18(1), 50–60. https://doi.org/10.1071/wf07072

Tang, W., Finney, M., McAllister, S., & Gollner, M. (2019). An Experimental Study of Intermittent Heating Frequencies From Wind-Driven Flames. *Frontiers in Mechanical Engineering*, *5*, 34. https://doi.org/10.3389/fmech.2019.00034

Wallace, J. M. (2016). Quadrant Analysis in Turbulence Research: History and Evolution. *Annual Review of Fluid Mechanics*, *48*(1), 131–158. https://doi.org/10.1146/annurev-fluid-122414-034550